Angewandte
International Edition Chemie

Controllable Optical Activity

DOI: 10.1002/anie.201305389

Controllable Optical Activity of Gold Nanorod and Chiral Quantum Dot Assemblies**

Zhening Zhu, Jun Guo, Wenjing Liu, Zhengtao Li, Bing Han, Wei Zhang, and Zhiyong Tang**

The controllable optical coupling between noble metal nanoparticles (NPs) and semiconductor quantum dots (QDs) is a challenging but very promising research topic owing to the great interest in the fundamental understanding of the exciton–plasmon interaction as well as the innovative applications in the fields of sensors,[1] bioimaging,[2] microelectronics,[3] and solar cells.[4] Currently, many exciting optical properties have been obtained with the assemblies composed of noble metal NPs and semiconductor QDs, and the corresponding results could be generally classified into two types: 1) The surface plasmon resonance (SPR) features of the noble metal NPs could be amplified or altered by the nearby QDs;[5] and 2) the photoluminescence of QDs is either quenched based on Förster resonance energy transfer (FRET) to the neighboring noble metal NPs, or enhanced by plasmon resonance excitation of the noble metal NPs.[6] Nevertheless, the study of the optical coupling in these assemblies is still in its infancy, for example, all of the reports are only focused on investigation of the UV/Vis absorption or photoluminescence characteristics of the assemblies. To explore new optical coupling properties is extremely important for both theory and applications of the noble metal–semiconductor nanohybrids.

A novel type of optical phenomenon, which is called as nanoscale optical activity, has been recently discovered.[7] As an example, when chiral organic molecules are close to Au NPs or Au nanorods (NRs), a new circular dichroism (CD) response appears at the wavelength of SPR band of Au NPs or NRs, while the original CD intensity of the chiral molecules is slightly enhanced.[8] Such chiral optical changes are attributed to optical coupling between chiral organic molecules and noble metal NPs.[9] However, the CD signals of the chiral organic molecules are normally located at the UV light region, and furthermore their CD wavelength is fixed and hard to be tuned, which makes study and manipulation of nanoscale optical activity become difficult. Fortunately, the latest studies have revealed that chiral QDs including chiral CdS, CdSe, and CdTe have size-dependent optical activity in the visible light region, and their CD peaks are red-shifted with increasing size.[10] Evidently, the assembly of noble metal NPs and semiconductor QDs will not only allow us to fully investigate the chiroptical properties caused by NP–NP interactions, but also provide the opportunities to accurately control the nanoscale optical activity.

Herein, we construct the binary assemblies containing Au NRs and chiral CdTe QDs and study their optical activity. The optical coupling between chiral QDs and Au NRs gives rise to generation of the plasmonic CD response of Au NRs and simultaneous enhancement of the CD intensity of QDs. Additionally, the coupled optical activity can be manipulated by changing either the aspect ratio of Au NRs or the size of QDs. The corresponding theoretical calculation result is consistent with the experimental observation.

Semiconductor QDs synthesized with chiral biomolecules exhibit a unique CD response in the visible light region.[10a] As for L-glutathione (L-GSH)-stabilized CdTe QDs, two CD peaks could be observed, a positive peak at 557 nm and a negative peak at 602 nm, near the first excitonic absorption band (FEAB) of CdTe QDs at 583 nm (dashed curve in Figure 1). Subsequently, the chiral QDs of negative surface

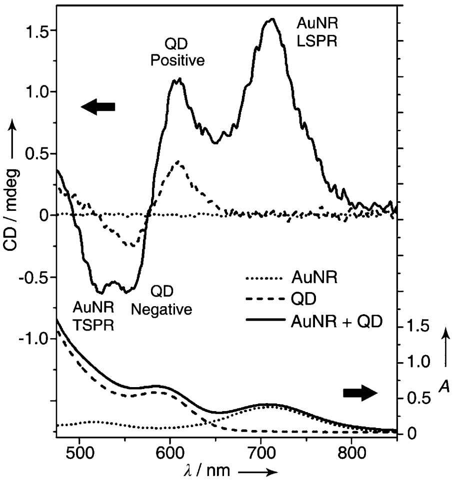

Figure 1. CD and absorption spectra of L-GSH-stabilized CdTe QDs (-----), Au NRs (•••••), and the assembly of Au NRs and CdTe QDs (——). The phrases "QD Negative" and "QD Positive" represent the negative CD and positive CD peaks of QDs, respectively, while the phrases "AuNR TSPR" and "AuNR LSPR" stand for the TSPR CD and LSPR CD peaks of Au NRs, respectively.

---

[*] Z. Zhu, J. Guo, W. Liu, Z. Li, B. Han, Prof. Z. Tang
Laboratory of Nanomaterials
National Center for Nanoscience and Technology
Beijing 100190 (P. R. China)
E-mail: zytang@nanoctr.cn
Prof. W. Zhang
Institute of Applied Physics and Computational Mathematics,
Beijing 100088 (P. R. China)
E-mail: zhang_wei@iapcm.ac.cn

[**] This work was partially supported by the National Key Basic Research Program of China (2014CB931801, Z.T.), the National Natural Science Foundation for Distinguished Youth Scholars of China (21025310, Z.T.), the National Natural Science Foundation of China (91027011, Z.T., 11174042, W.Z.), and the National Basic Research Program of China (2011CB922204, W.Z.).

Supporting information for this article is available on the WWW under http://dx.doi.org/10.1002/anie.201305389.

charges are assembled surrounding the positively charged AuNRs through electrostatic attraction, resulting in reversion of the surface charges of AuNRs (Supporting Information, Figures S1–S3). Notably, two concomitant CD response changes are clearly discerned after formation of the assembly. First, in respect to pure AuNRs and CdTe QDs, two new CD peaks appear at 521 nm and 711 nm, respectively (Figure 1 top, solid curve). Previous studies have demonstrated that the chiral molecules could induce generation of plasmonic CD response of AuNPs.[11] Similarly, the chiral dipoles of CdTe QDs near the AuNR surface would also create the chiral current inside AuNRs, leading to the transportation of chirality from CdTe QDs to AuNRs. The two new CD peaks should be assigned to the transverse SPR (TSPR, absorption peak at 519 nm) and longitudinal SPR (LSPR, absorption peak at 711 nm) of AuNRs (dotted curve in bottom Figure of Figure 1), respectively, which are called TSPR CD and LSPR CD herein. Second, comparing with pure QDs of the same concentration, the intensity of both CD peaks of L-GSH stabilized CdTe at 555 nm and 602 nm is considerably increased (Figure 1 top, solid curve), and the enhanced multiples are calculated to be 1.76 and 2.39, respectively. It is well known that the SPR features of AuNRs could bring about the strong surface electromagnetic fields, which remarkably influence the optical activity of CdTe QDs in proximity to the AuNRs. As a result, the CD intensity of the QDs is obviously increased. The above two phenomena indicate the coupling optical activity between AuNRs and chiral QDs in the assembly. The contrast experiment by mixture of AuNRs and pure L-GSH further confirms that the unique plasmonic CD of AuNRs results from coupling between AuNRs and chiral QDs rather than interaction between AuNRs and chiral molecules (Supporting Information, Figure S4).

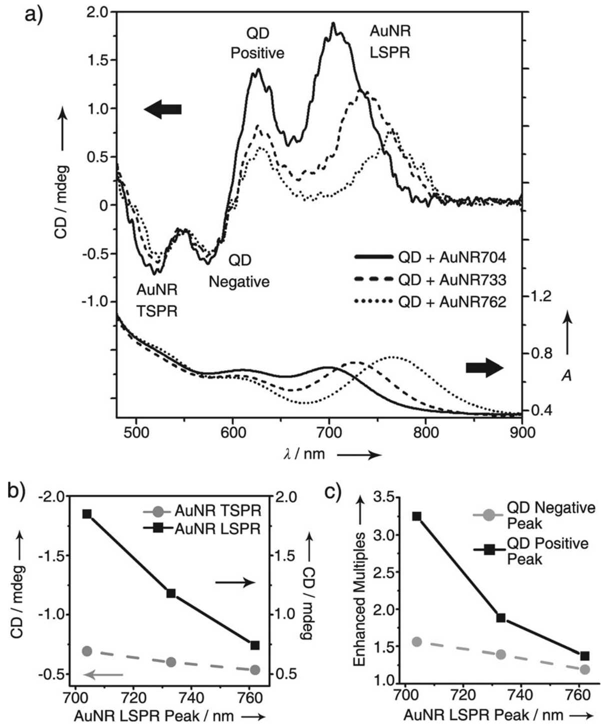

Figure 2. a) CD and adsorption spectra of the assemblies with changing the aspect ratio of AuNRs; b) TSPR CD response (-----) and LSPR CD response (——) of AuNRs against their LSPR peak position; c) intensity change by the enhanced multiples of the negative CD peak (-----) and the positive CD peak (——) of the CdTe QDs against the LSPR peak position of AuNRs. Note: The numbers in (a) represent the LSPR wavelengths of different AuNRs; for example, "AuNR704" stands for AuNRs with the LSPR wavelength at 704 nm.

As the SPR characteristics of Au NRs can be manipulated by changing their aspect ratio, the question naturally arises as to whether we may control the optical activity of the assemblies by alternation of the aspect ratio of AuNRs. To answer this question, three types of AuNRs with their LSPR absorbance peaks centered at 704, 733, and 762 nm, respectively (Supporting Information, Figures S5–S7), are used as the building blocks to integrate with the same CdTe QDs of the FEAB at 599 nm (Figure 2a; Supporting Information, Figure S8). It is clear that following the shift of the LSPR peaks of AuNRs to the longer wavelength, the LSPR CD peaks are also red-shifted from 704 nm to 762 nm with a dramatic decrease of the CD intensity (Figure 2a, solid line in Figure 2b; Supporting Information, Table S1), while the TSPR CD peaks at about 520 nm exhibit an only slight decrease of the CD intensity (Figure 2a, dashed line in Figure 2b; Supporting Information, Table S1). Typically, when the AuNRs are of the same concentration in the solution, their LSPR absorbance intensity is increased with the bathochromic shift of the peak position, which is supposed to result in the enhanced LSPR CD response of AuNRs (Supporting Information, Figure S5).[12] However, as the LSPR absorbance moves to the longer wavelength, the plasmon frequency of AuNRs is farther away from the FEAB of CdTe QDs (599 nm), leading to a weaker coupling effect (Figure 2a). The LSPR CD intensity is obviously decreased with the red-shift of the LSPR peak position of AuNRs (solid line in Figure 2b), suggesting that the absorbance peak positions of AuNRs and CdTe QDs rather than the AuNR SPR intensity are dominant for plasmoinc CD response of AuNRs. As comparison, when the aspect ratio of AuNRs is increased, the peak position of the TSPR absorbance of AuNRs is kept unchanged at about 520 nm, with a slight decrease of the peak intensity (Supporting Information, Figure S5). Therefore, the TSPR CD response of Au NRs only shows slight decrease (dashed line in Figure 2b).

Analogously, the optical activity of chiral CdTe QDs is also influenced by the coupling effect in presence of AuNRs. As the LSPR absorbance of AuNRs moves to a longer wavelength, its coupling with the adjacent positive CD peak of CdTe QDs at 625 nm is weakened, so the enhanced multiples of the corresponding CD response of QDs are considerably decreased from 3.25 to 1.37 (Figure 2a, solid line in Figure 2c; Supporting Information, Table S2). As a comparison, the change is not obvious for the enhanced multiples of the negative CD peak of CdTe QDs (ca. 566 nm) that is close to the TSPR peak of AuNRs (ca. 520 nm). Because the TSPR absorbance shows unchanged peak position and slight decrease of peak intensity with the increase of the aspect ratio of AuNRs, it is reasonable that the change in the enhanced multiples of the negative CD peaks of QDs is relatively small, from 1.56 to 1.19 (Figure 2a, dashed line in Figure 2c; Supporting Information, Table S2). Again, the absorbance peak position rather than the absorbance intensity dominates the optical coupling between AuNRs and chiral CdTe QDs in the assembly.

As the chiral QDs can exhibit size-dependent optical activity as we previously reported,[10a] another question is directed to whether we could manipulate the coupling between AuNRs and QDs by changing the size of CdTe QDs. We select three types of L-GSH-stabilized CdTe QDs with their FEAB centered at 564 nm, 586 nm, and 608 nm, respectively, and CD measurement confirms that these QDs exhibit the size-dependent optical activity (Supporting Information, Figure S10). The above CdTe QDs are, respectively, assembled with the same AuNRs of the LSPR absorbance peak at 711 nm (Supporting Information, Figure S11). As the size of QDs increases, the FEAB peak of CdTe QDs and the LSPR absorbance peak of AuNRs approach one another, giving rise to both enhancement of the positive CD peak of QDs (Figure 3a, solid line in Figure 3b; ; SI,, Table S3) and the LSPR CD peak of AuNRs (Figure 3a, solid line in Figure 3c; Supporting Information, Table S4); on the contrary, the FEAB peak of CdTe QDs and the TSPR absorbance peak of AuNRs are gradually separating with increasing QD size, and thus the intensity of both the negative CD peak of CdTe QDs and the TSPR CD peak of AuNRs is reduced (Figure 3a, dashed line in Figure 3b and Figure 3c; Supporting Information, Tables S3, S4). This result is similar to that obtained with alternation of the AuNR aspect ratio, suggesting that tuning the optical absorbance of AuNRs and CdTe QDs are equally significant and efficient for manipulation of the coupling optical activity inside the assemblies.

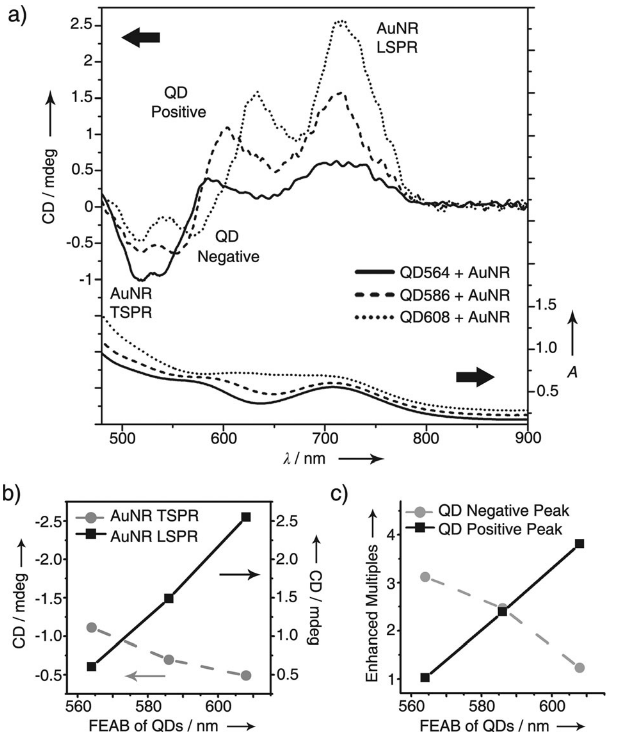

Figure 3. a) CD and absorption spectra of the assemblies with changing the size of QDs; b) TSPR CD (-----) and LSPR CD (——) responses against the first excitonic absorption band (FEAB) of CdTe QDs; c) intensity change by the enhanced multiples of the negative peak (-----) and the positive peak (——) of the CdTe QDs. Note: The numbers in (a) represent the FEAB of different QDs; for example, "QD564" stands for the QDs with the FEAB centered at 564 nm.

Finally, a semi-quantitative theory is developed to further understand the tunable interaction between chiral CdTe QDs and AuNRs in the assembly. Here the chirality of CdTe QDs originates from the optical coupling between the chiral capping agents and QD cores, and the size dependent absorbance features of QDs cause the tunable CD response. Meanwhile, the optical absorbance characteristics of AuNRs can also be tuned by changing their aspect ratio. The interaction between QDs and AuNRs, which results in many interesting optical properties, depends mainly on the geometrical arrangement and the spectrum feature of CdTe QDs and AuNRs. The definition of CD is the difference of optical absorption (Q) between left and right circularly polarized light, that is, $CD = Q^L - Q^R$, where:[5c,13]

$$Q^{L/R} = Q^{L/R}_{\mathrm{QD}} + Q^{L/R}_{\mathrm{AuNR}} \tag{1}$$

$$Q^{L/R}_{\mathrm{QD}} = \omega \mathrm{Im}[\tilde{\alpha}^{L/R}] |E_{\mathrm{QD}}|^2 \tag{2}$$

$$Q_{\mathrm{AuNR}} = \frac{\omega \varepsilon_0^2 Im[\varepsilon_1]}{|(1-L)\varepsilon_0 + L\varepsilon_1|^2} N_{\mathrm{AuNR}} V_{\mathrm{AuNR}} |E_{\mathrm{AuNR}}|^2 \tag{3}$$

In Equations (2) and (3),

$$\tilde{\alpha}^{L/R} = \tilde{\alpha}_0 \pm \Delta\tilde{\alpha} = (\alpha_0 \pm \Delta\alpha_0) V_{\mathrm{QD}} N_{\mathrm{QD}} \tag{4}$$

where the polarizability of QD for left/right circularly polarized field is given by $\alpha_0{}^{L/R} = \alpha_0 \pm \Delta\alpha_0$ (that is, α_0 and $2\Delta\alpha_0$ are the average and difference of the polarizabilities of QD for left and right circularly polarized light), V_{QD} and N_{QD} are the volume and number of QDs, V_{AuNR} and N_{AuNR} are the volume and number of AuNRs, ω is the frequency of the incident light, ε_0 and ε_1 are the dielectric constants of background and bulk Au, L is the geometric factor of AuNRs, and E_{QD} and E_{AuNR} are the local fields on CdTe QDs and AuNRs, respectively. The local fields E_{QD} and E_{AuNR} can be obtained by solving the self-consistent coupled equations (for detailed calculations, see the Supporting Information). Therefore, we arrive at the following equations:

$$CD_{\mathrm{QD}} = \frac{\omega |1+\gamma|^2 E_0^2}{|1-\bar{\alpha}\gamma|^2} \left\{ \mathrm{Im}[\Delta\tilde{\alpha}] + 2\mathrm{Im}[\tilde{\alpha}_0] \mathrm{Re}\left[\frac{\Delta\alpha\gamma}{1-\bar{\alpha}\gamma}\right] \right\} \tag{5}$$

$$CD_{\mathrm{AuNR}} = \frac{\omega \varepsilon_0^2 \mathrm{Im}[\varepsilon_1] E_0^2}{|(1-L)\varepsilon_0 + L\varepsilon_1|^2} \frac{N_{\mathrm{AuNR}} V_{\mathrm{AuNR}}}{|1-\bar{\alpha}\gamma|^2} 2\mathrm{Re}[1+\bar{\alpha}]^* \frac{(1+\gamma)\Delta\alpha}{1-\bar{\alpha}\gamma} \tag{6}$$

where:

$$\alpha_{L/R} = \bar{\alpha} \pm \Delta\alpha = (\tilde{\alpha}_0 \pm \Delta\tilde{\alpha}) G = \tilde{\alpha}^{L/R} G \tag{7}$$

G is the strength of coupling between an AuNR and a QD, $\gamma = G V_{\mathrm{AuNR}} \gamma_0$, $\gamma_0 = (\varepsilon_0 - \varepsilon_1)/[(1L)\varepsilon_0 + L\varepsilon_1]$.

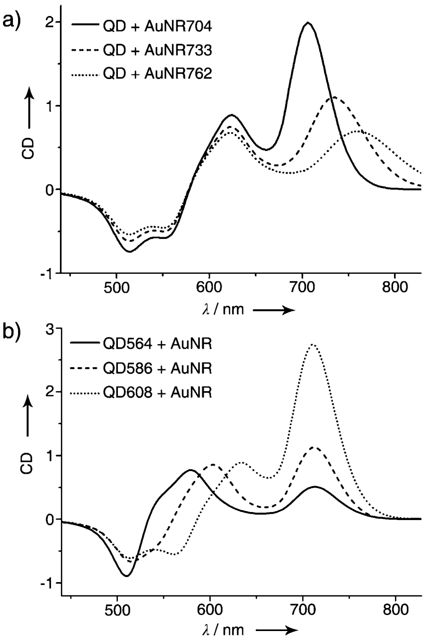

Figure 4. Corresponding theoretical modeling for the optical activity of the assemblies when a) changing the aspect ratio of Au NRs or b) changing the size of QDs.

The total CD spectrum is the sum of CD signals of the Au NRs and CdTe QDs in the assembly of the different configurations and with the incident field of different polarizations.

Figure 4 shows the result of the calculations, and several important conclusions could be drawn. First, it is clear that the CD response of the chiral CdTe QDs can be tuned by changing the size of QDs (Figure 4 b) and enhanced by the Au NRs (Figure 4 a). This is understood considering that $CD_{\mathrm{QD}} \propto \omega|1+\gamma|^2E_0^2\mathrm{Im}[\Delta\tilde{\alpha}]$ (to the first order of G) and $|1+\gamma|^2$ is the field enhancement factor in the presence of Au NRs. Second, based on $CD_{\mathrm{AuNR}} \propto \mathrm{Re}[\Delta\alpha]/|(1L)\varepsilon_0+L\varepsilon_1|^2$ (to the first order of G), it can be deduced that the CD response of Au NRs is induced by QDs ($\propto \mathrm{Re}[\Delta\alpha]$) and can be tuned by the geometry (aspect ratio) of Au NRs ($\propto 1/|(1L)\varepsilon_0+L\varepsilon_1|^2$; Figure 4 a). Last but not least, as shown in Figure 4, the coupling effect becomes stronger when the CD peak of CdTe QDs is closer to the plasmon peak of Au NRs. Notably, the quantitative comparison on the CD intensity and the corresponding enhanced multiples demonstrates good agreement between theoretical calculation and the experimental result (Supporting Information, Tables S5, S6), which highlights the fact that the near-field interaction between noble metal NRs and semiconductor QDs leads to enhancement of CD signals of chiral QDs and simultaneous generation of the plasmon induced CD of noble metal NRs.

In summary, we studied the coupling optical activity between Au NRs and chiral CdTe QDs in an assembly. Both experimental result and theoretical calculation demonstrate that the coupling is well-controllable by manipulating either the SPR absorbance of Au NRs or the excitonic absorbance of QDs. Better results can be obtained by using more monodispersed QDs and continuously tunable Au NRs.[14] To the best of our knowledge, this is the first report on the systematic investigation of the coupling optical activity of the assemblies made of noble metal nanoparticles and semiconductor QDs with different nature, which provides us quantitative understanding of key factors to influence the optical activity of nanoscale composites. The work will give a new insight into the noble metal–semiconductor NP coupled system and provide a novel route to tune the nanoscale optical activity, which have many potential applications in metamaterials, circular polarizers, and sensors.[15]

Received: June 23, 2013
Published online: November 7, 2013

Keywords: chirality · gold nanorods · optical activity · quantum dots · surface plasmon resonance

---

[1] a) Y. Shan, J. Xu, H. Chen, *Chem. Commun.* **2009**, 905 – 907; b) L. Song, S. Wang, N. A. Kotov, Y. Xia, *Anal. Chem.* **2012**, *84*, 7330 – 7335.

[2] a) N. Erathodiyil, J. Ying, *Acc. Chem. Res.* **2011**, *44*, 925 – 935; b) Y. Jin, X. Gao, *Nat. Nanotechnol.* **2009**, *4*, 571 – 576.

[3] H. Meng, Y. Yang, Y. Chen, Y. Zhou, Y. Liu, X. Chen, H. Ma, Z. Tang, D. Liu, L. Jiang, *Chem. Commun.* **2009**, 2293 – 2295.

[4] H. A. Atwater, A. Polman, *Nat. Mater.* **2010**, *9*, 205 – 213.

[5] a) D. J. Bergman, M. I. Stockman, *Phys. Rev. Lett.* **2003**, *90*, 027402; b) W. Zhang, A. O. Govorov, *Phys. Rev. B* **2011**, *84*, 081405; c) W. Zhang, A. O. Govorov, G. W. Bryant, *Phys. Rev. Lett.* **2006**, *97*, 146804.

[6] a) O. Kulakovich, N. Strekal, A. Yaroshevich, S. Maskevich, S. Gaponenko, I. Nabiev, U. Woggon, M. Artemyev, *Nano Lett.* **2002**, *2*, 1449 – 1452; b) J. Lee, A. O. Govorov, J. Dulka, N. A. Kotov, *Nano Lett.* **2004**, *4*, 2323 – 2330; c) E. Oh, M. Y. Hong, D. Lee, S. H. Nam, H. C. Yoon, H. S. Kim, *J. Am. Chem. Soc.* **2005**, *127*, 3270 – 3271; d) E. Cohen-Hoshen, G. W. Bryant, I. Pinkas, J. Sperling, I. Bar-Joseph, *Nano Lett.* **2012**, *12*, 4260 – 4264.

[7] Y. Wang, J. Xu, Y. Wang, H. Chen, *Chem. Soc. Rev.* **2013**, *42*, 2930 – 2962.

[8] A. O. Govorov, Z. Fan, P. Hernandez, J. M. Slocik, R. R. Naik, *Nano Lett.* **2010**, *10*, 1374 – 1382.

[9] a) I. Lieberman, G. Shemer, T. Fried, E. M. Kosower, G. Markovich, *Angew. Chem.* **2008**, *120*, 4933 – 4935; *Angew. Chem. Int. Ed.* **2008**, *47*, 4855 – 4857; b) A. Guerrero-Martínez, B. Auguie, J. L. Alonso-Gomez, Z. Dzolic, S. Gomez-Grana, M. Zinic, M. M. Cid, L. M. Liz-Marzan, *Angew. Chem.* **2011**, *123*, 5613 – 5617; *Angew. Chem. Int. Ed.* **2011**, *50*, 5499 – 5503; c) H. Q. Qi, K. E. Shopsowitz, W. Y. Hamad, M. J. MacLachlan, *J. Am. Chem. Soc.* **2011**, *133*, 3728 – 3731.

[10] a) Y. Zhou, Z. Zhu, W. Huang, W. Liu, S. Wu, X. Liu, Y. Gao, W. Zhang, Z. Tang, *Angew. Chem.* **2011**, *123*, 11658 – 11661; *Angew. Chem. Int. Ed.* **2011**, *50*, 11456 – 11459; b) A. Ben Moshe, D. Szwarcman, G. Markovich, *ACS Nano* **2011**, *5*, 9034 – 9043.

[11] a) Z. Zhu, W. Liu, Z. Li, B. Han, Y. Zhou, Y. Gao, Z. Tang, *ACS Nano* **2012**, *6*, 2326 – 2332; b) Z. Li, Z. Zhu, W. Liu, Y. Zhou, B. Han, Y. Gao, Z. Tang, *J. Am. Chem. Soc.* **2012**, *134*, 3322 – 3325; c) J. George, K. G. Thomas, *J. Am. Chem. Soc.* **2010**, *132*, 2502 – 2503.

[12] C. J. Orendorff, C. J. Murphy, *J. Phys. Chem. B* **2006**, *110*, 3990 – 3994.

[13] a) H. Haug, S. W. Koch, *Quantum Theory of the Optical and Electronic Properties of Semiconductors*, World Scientific Publishing, Singapore, **2004**; b) C. F. Bohren, D. R. Huffman,

Absorption and Scattering of Light by Small Particles, Wiley, New York, **1983**.

[14] K. C. Ng, W. Cheng, *Nanotechnology* **2012**, *23*, 105602.

[15] a) F. J. Heiligtag, M. D. Rossell, M. J. Suess, M. Niederberger, *J. Mater. Chem.* **2011**, *21*, 16893 – 16899; b) Z. Nie, A. Petukhova, E. Kumacheva, *Nat. Nanotechnol.* **2010**, *5*, 15 – 25; c) T. Wang, D. LaMontagne, J. Lynch, J. Zhuang, Y. Cao, *Chem. Soc. Rev.* **2013**, *42*, 2804 – 2823; d) S. Tan, M. J. Campolongo, D. Luo, W. Cheng, *Nat. Nanotechnol.* **2011**, *6*, 268 – 276.